Classical Diagram Technique for Calculating Thermostatic Properties of Solids; Application to Dielectric Susceptibility of Paraelectrics

R. M. WILCOX
National Bureau of Standards, Boulder Laboratories, Boulder, Colorado
(Received 5 January 1965; revised manuscript received 17 March 1965)

A diagram technique suitable for calculating equilibrium classical statistical properties of solid dielectrics is developed. The method is applied to the temperature-dependent dielectric susceptibility and vibration spectrum of an anharmonic crystal. The techniques of "diagram summation" and "frequency renormalization" are used to obtain a Curie-law formula for the susceptibility of paraelectric materials. The method is extended to obtain a new formula for the susceptibility in the presence of a biasing field. Some possible applications of the theory to relevant experiments are mentioned.

I. INTRODUCTION

SINCE their inception by Mayer[1] in 1937, diagram techniques have been developed by many workers to provide a powerful tool for the solution of various problems of theoretical physics. A significant recent application of these techniques is the quantum-statistical treatment given by Cowley[2] of the normal-mode frequencies, elastic constants, thermal expansion coefficient, free energy, frequency-dependent dielectric constant, and other thermodynamic properties of an anharmonic crystal. The present paper fills an apparent need by developing specifically for classical equilibrium statistical mechanics a diagram technique closely analogous to Cowley's general theory. Although such results can always be obtained from Cowley's theory as a limiting case, the present paper avoids sophisticated operator, complex-variable, and Fourier-transform techniques, as well as a lot of messy algebra, but retains the advantages of the diagram method. It is hoped therefore that this paper will not only help more readers to comprehend diagram techniques, but will also provide a basis for answering certain kinds of questions with greater ease than can be done with the more general theories.

We restrict ourselves to thermostatic properties since even a classical treatment[3] of nonequilibrium properties appears to involve considerable complication. Despite the obvious limitations of the present theory, there is still a fairly large class of problems where it may be usefully employed. In particular, it should be applicable to the calculation of thermostatic properties of dielectrics at temperatures above the Debye temperature, where factors other than quantum statistics are most relevant.

This paper is confined to a treatment of the static dielectric-susceptibility tensor $\chi^{\alpha\beta}$ and its relationship with the lattice-vibrational spectrum. Other thermostatic properties, such as the elastic constants, expansion coefficient, and free energy, can of course be obtained by similar methods. In Sec. II $\chi^{\alpha\beta}$ is defined and expressed in terms of thermal averages of lattice-dynamical quantities. In Sec. III a diagram technique for the perturbation expansion of $\chi^{\alpha\beta}$ is introduced. All zero- and first-order contributions in powers of the absolute temperature are calculated. In Sec. IV the techniques of "diagram summation" and "renormalization" are employed to obtain the Curie-law formula characteristic of paraelectrics. In Sec. V the calculation is extended to obtain a new formula for the susceptibility tensor $\chi^{\alpha\beta}(\mathbf{E})$ in the presence of a biasing field $\mathbf{E}$. If the field $\mathbf{E}$ is not too large, the result reduces to a formula of the Slater theory, but the assumptions of that theory are considerably more restrictive than those of the present theory.

II. THE DIELECTRIC SUSCEPTIBILITY OF AN ANHARMONIC SOLID

According to the adiabatic approximation,[4] well suited to an insulating solid at all lattice frequencies, the electronic wave function of a crystal is uniquely determined by the instantaneous positions of all the nuclei, while the nuclei move in a potential determined by their mutual Coulomb interactions and by the electronic charge density. The potential energy U and the dipole moment $\mathbf{M}$ of the crystal are thus completely determined by the positions of the nuclei. The potential energy of the crystal in a constant applied field $\mathbf{E}$ is thus

$$U(\mathbf{E}) \equiv U - \mathbf{E}\cdot\mathbf{M}. \tag{1}$$

The thermal average of the dipole moment of a canonical ensemble in the classical-statistical approximation is given by

$$\langle \mathbf{M} \rangle_E \equiv \int \mathbf{M} e^{-\beta U(\mathbf{E})} d\tau \Big/ \int e^{-\beta U(\mathbf{E})} d\tau, \tag{2}$$

where $d\tau$ is the configuration-space volume element and $1/\beta \equiv k_B T$, as usual. The macroscopic polarization vector $\mathbf{P}$ is identified with the dipole moment per unit volume,

[1] J. E. Mayer, J. Chem. Phys. **5**, 67, 74 (1937); J. E. Mayer and M. G. Mayer, *Statistical Mechanics* (John Wiley & Sons, Inc., New York, 1940), Chap. 13.
[2] R. A. Cowley, Advan. Phys. **12**, 421 (1963). This paper extends a method due to A. A. Maradudin and A. E. Fein, Phys. Rev. **128**, 2589 (1962).
[3] I. Prigogine, *Non-Equilibrium Statistical Mechanics* (Interscience Publishers, Inc., New York, 1962).
[4] M. Born and K. Huang, *Dynamical Theory of Crystal Lattices* (Oxford University Press, New York, 1954), Chap. IV.

so that

$$\mathbf{P}\equiv\tau^{-1}\langle\mathbf{M}\rangle_E, \tag{3}$$

where τ is the volume of the crystal. The field-dependent susceptibility tensor $\chi^{\alpha\beta}(\mathbf{E})$ is here defined by[5]

$$\chi^{\alpha\beta}(\mathbf{E})\equiv\partial P^\alpha/\partial E^\beta, \quad (\alpha,\beta=x,y,z). \tag{4}$$

From Eqs. (2), (3), and (4), it follows that

$$\chi^{\alpha\beta}(\mathbf{E})=(\beta/\tau)[\langle M^\alpha M^\beta\rangle_E-\langle M^\alpha\rangle_E\langle M^\beta\rangle_E], \tag{5}$$

$$=(\beta/\tau)\langle\Delta M^\alpha\Delta M^\beta\rangle_E, \tag{5a}$$

where $\Delta\mathbf{M}\equiv\mathbf{M}-\langle\mathbf{M}\rangle_E$.[6] In the weak-field limit, $\mathbf{E}\rightarrow\mathbf{0}$,[7]

$$\chi^{\alpha\beta}\equiv\chi^{\alpha\beta}(\mathbf{0})=(\beta/\tau)[\langle M^\alpha M^\beta\rangle-\langle M^\alpha\rangle\langle M^\beta\rangle], \tag{6}$$

$$=(\beta/\tau)\langle\Delta M^\alpha\Delta M^\beta\rangle. \tag{6a}$$

To evaluate the ensemble averages, it is convenient to use complex normal coordinates A_λ. We do not here consider the method for transforming to or from such coordinates, since this is given elsewhere,[4,8] but merely state formulas for the potential and dipole moment, respectively:

$$U=H+V, \tag{7}$$

$$H\equiv\tfrac{1}{2}\textstyle\sum_\lambda\omega_\lambda^2A_\lambda^*A_\lambda, \tag{7a}$$

$$V=V_3+V_4+\cdots, \tag{7b}$$

$$V_3=\sum_{\lambda\lambda'\lambda_2}\Delta(\mathbf{k}+\mathbf{k}'+\mathbf{k}_2)V_3(\lambda\lambda'\lambda_2)A_\lambda A_{\lambda'}A_{\lambda_2}, \tag{7c}$$

$$V_4=\sum_{\lambda\lambda'\lambda_2\lambda_3}\Delta(\mathbf{k}+\mathbf{k}'+\mathbf{k}_2+\mathbf{k}_3)\times V_4(\lambda\lambda'\lambda_2\lambda_3)A_\lambda A_{\lambda'}A_{\lambda_2}A_{\lambda_3}, \tag{7d}$$

$$\mathbf{M}=\mathbf{M}_0+\mathbf{M}_1+\mathbf{M}_2+\mathbf{M}_3+\cdots, \tag{8}$$

$$\mathbf{M}_0\equiv\text{const}, \tag{8a}$$

$$\mathbf{M}_1\equiv\textstyle\sum_j\mathbf{M}_{1j}A_j, \tag{8b}$$

$$\mathbf{M}_2\equiv\sum_{\lambda\lambda'}\Delta(\mathbf{k}+\mathbf{k}')\mathbf{M}_2(\lambda\lambda')A_\lambda A_{\lambda'}, \tag{8c}$$

$$\mathbf{M}_3\equiv\sum_{\lambda\lambda'\lambda_2}\Delta(\mathbf{k}+\mathbf{k}'+\mathbf{k}_2)\mathbf{M}_2(\lambda\lambda'\lambda_2)A_\lambda A_{\lambda'}A_{\lambda_2}. \tag{8d}$$

The symbols λ, λ', etc., are condensed notation for $(\mathbf{k}j)$, $(\mathbf{k}'j')$ etc., respectively, where $\mathbf{k}$, $\mathbf{k}'$, etc., are wave vectors of the reciprocal lattice and j, j', etc., designate particular branches of the spectrum. We will use the convention that if a j appears alone, as in Eq. (8b), it is an optical mode for which $\mathbf{k}=\mathbf{0}$. The summations over λ, λ', etc., are over all normal modes in the first Brillouin zone. The Δ functions ensure wave-vector conservation since $\Delta(\mathbf{k})\equiv0$, unless $\mathbf{k}=\mathbf{0}$ modulus, a translation vector of the reciprocal lattice, in which case $\Delta(\mathbf{k})\equiv1$. The quantities $V_3(\lambda\lambda'\lambda_2)$, $V_4(\lambda\lambda'\lambda_2\lambda_3)$, $\mathbf{M}_2(\lambda\lambda')$, and $\mathbf{M}_3(\lambda\lambda'\lambda_2)$ are defined to be completely symmetric with respect to interchanges of λ's. The A_λ are not completely independent since they satisfy

$$A_{-\lambda}=A_\lambda^*, \tag{9}$$

where $-\lambda$ stands for $(-\mathbf{k}j)$.

From Eq. (7), the calculation of Eq. (6) reduces to a calculation of the quantities

$$\langle\mathbf{M}\rangle=(e^{-\beta V}\mathbf{M})/(e^{-\beta V}) \tag{10}$$

and

$$\langle M^\alpha M^\beta\rangle=(e^{-\beta V}M^\alpha M^\beta)/(e^{-\beta V}), \tag{11}$$

where we use parentheses to denote harmonic-potential-ensemble averages for any quantity Q:

$$(Q)\equiv\int Qe^{-\beta H}d\tau\Big/\int e^{-\beta H}d\tau. \tag{12}$$

III. THE DIAGRAM METHOD

By expanding $e^{-\beta V}$ in its power series, and using Eqs. (7), (8), and (12), we see that Eqs. (10) and (11) reduce to calculating harmonic-ensemble averages of A_λ products

$$(\lambda_1\lambda_2\cdots\lambda_n)\equiv(A_{\lambda1}A_{\lambda2}\cdots A_{\lambda n}). \tag{13}$$

Note that $(\lambda_1\lambda_2\cdots\lambda_n)$ is completely symmetric with respect to interchange of indices. It is shown in Appendix A that the quantity occurring in Eq. (13), named a *hafnian* by Caianiello,[9] satisfies

$$(\lambda_1\lambda_2\cdots\lambda_{2n-1})\equiv0, \tag{14a}$$

$$(\lambda_1\lambda_2\cdots\lambda_{2n})\equiv\textstyle\sum_P(\lambda_{i1}\lambda_{i2})(\lambda_{i3}\lambda_{i4})\cdots(\lambda_{i2n-1}\lambda_{i2n}), \tag{14b}$$

where

$$\begin{aligned}(\lambda\lambda')&\equiv0, && \lambda\neq-\lambda'\\ &\equiv1/(\beta\omega_\lambda^2), && \lambda=-\lambda'.\end{aligned} \tag{14c}$$

[5] Note that $\chi^{\alpha\beta}(\mathbf{E})$ depends upon the sample shape since the $\mathbf{E}$ occurring in Eq. (1) is the applied field, not necessarily the macroscopic field. The relationship of $\chi^{\alpha\beta}(\mathbf{E})$ to the ordinary shape-independent dielectric susceptibility is, in general, a problem in electrostatics. If, following Szigeti (Ref. 17), the sample is chosen to be a thin slab parallel to the applied field, the macroscopic field is the same as the applied field and $\chi^{\alpha\beta}(\mathbf{E})$ is then the shape-independent susceptibility. Alternatively, $\chi^{\alpha\beta}(\mathbf{E})$ will be shape-independent with $\mathbf{E}$ the macroscopic field if the potential U in Eq. (1) is redefined appropriately. Born and Huang's book (Ref. 4) shows how this may be done. We will assume that either of the last two procedures is employed so that henceforth $\mathbf{E}$ will stand for the macroscopic field.

[6] Our treatment here is actually slightly oversimplified since we have neglected the influence of the applied field in causing the electron cloud to shift relative to the nuclei. A more rigorous treatment (R. M. Wilcox, to be published) shows that Eq. (5) is still obtained as a good approximation for the so-called "infrared" contribution to the susceptibility tensor. The main approximation made is that the polarization due to the electron-cloud shift relative to the nuclei is independent of the positions of the nuclei.

[7] Equation (6a) shows a connection between the dielectric susceptibility and the statistical fluctuations of the dipole moment in the *absence* of an applied field. See H. Fröhlich, *Theory of Dielectrics* (Oxford University Press, New York, 1958), 2nd ed., Sec. 7.

[8] See J. M. Ziman, *Electrons and Phonons* (Oxford University Press, New York, 1960), Secs. 1.6, 3.2.

[9] E. R. Caianiello, Nuovo Cimento **10**, 1639 (1953).

In Eq. (14b), $i_1, i_2, i_3, \cdots, i_{2n}$ is any rearrangement of the integers $1, 2, \cdots, 2n$ subject to the restrictions $i_1<i_3<i_5<\cdots<i_{2n-1}$, $i_1<i_2$, $i_3<i_4, \cdots, i_{2n-1}<i_{2n}$, and the summation is over all such permutations. The quantity $(\lambda\lambda')$ is called a *contraction symbol.*

The numerators and denominators of Eqs. (10) and (11) may thus be written as a sum of terms in which each term corresponds to a *diagram*[10] as follows. Each term is a product of $\mathbf{M}_p$ or V_p factors Eqs. (7) and (8) multiplied by a term of the hafnian expansion Eq. (14b). To each $\mathbf{M}_p(\lambda_1\cdots\lambda_p)$ or $V_p(\lambda_1\cdots\lambda_p)$ factor appearing in the term, we associate a *vertex* terminating exactly p *mode lines.* A mode line λ represents the contraction symbol Eq. (14c)

$$g_\lambda \equiv (-\lambda\lambda) = k_B T/\omega_\lambda^2, \tag{15}$$

and connects a vertex with an index λ to a vertex with an index $-\lambda$. This requirement will be automatically satisfied if we label each line with an arrow in the direction of its $\mathbf{k}$ vector, and agree to the convention that a $\mathbf{k}$ vector directed *away* from a vertex corresponds to an index λ at that vertex (so that a $\mathbf{k}$ vector directed *towards* a vertex corresponds to an index $-\lambda$ at that vertex). Wave-vector conservation at each vertex then requires that the vector sum of the wave vectors leaving (or entering) a vertex be zero. To each term we can thus draw a corresponding diagram. Conversely, to each diagram which can be drawn according to the above rules, there will be a term of the perturbation expansion. However, in general, many of the diagrams which correspond to different terms will be *topologically equivalent*, i.e., they correspond to terms which are the same when the unessential difference between equivalent dummy λ indices is disregarded. In doing perturbation theory by the diagram method, one thus draws all possible *topologically inequivalent* diagrams of interest and calculates each diagram according to the above rules. Each diagram is then multiplied by an integer equal to the number of terms of the expansion which corresponds to the same diagram. Although it is possible to give precise rules for calculating this number, we prefer to show how this is obtained in the examples which we consider later. Also, each diagram has to be multiplied by a factor $(-\beta)^n/n!$ where n is the *order* of the diagram ($\equiv$the number of *internal vertices*$\equiv$the number of V_p vertices occurring in the diagram). (The $\mathbf{M}_p$ vertices are called *external vertices* since they do not arise from the expansion of $e^{-\beta V}$.) Hence a diagram of order n with l lines is proportional to T^{l-n}.

A diagram contributing to the numerator or denominator of Eq. (10) or (11) is said to be *linked* if each internal vertex connects directly or indirectly to an external vertex. Otherwise, it is said to be *unlinked.* It is shown in Appendix B that the quantities $\langle\mathbf{M}\rangle$ and $\langle M^\alpha M^\beta\rangle$ Eqs. (10) and (11) are composed of only linked diagrams with one and two external vertices, respectively. From Eq. (6) it is seen that $\chi^{\alpha\beta}$ is proportional to the difference of $\langle M^\alpha M^\beta\rangle$ and $\langle M^\alpha\rangle\langle M^\beta\rangle$. Now all of the diagrams occurring in $\langle M^\alpha\rangle\langle M^\beta\rangle$ also occur in $\langle M^\alpha M^\beta\rangle$ but not vice versa.[11] These are linked but *disconnected* diagrams, since M^α does not connect even indirectly to M^β. (A *connected* diagram is one in which each vertex connects directly or indirectly to *every* other vertex.) Hence only connected diagrams contribute to $\chi^{\alpha\beta}$.[12] That this must be the case is evident also from Eq. (6) on dimensional grounds since $\langle M^\alpha\rangle\langle M^\beta\rangle$ is proportional to τ^2 while $\chi^{\alpha\beta}$, an intensive quantity, is independent of τ.

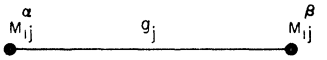

FIG. 1. A zeroth-order diagram, the only contribution to $\chi_0^{\alpha\beta}$.

The lowest order diagram which contributes to the susceptibility is shown in Fig. 1. It is simply a single line (factor $g_j \equiv (\beta\omega_j^2)^{-1}$) connecting the two external vertices $M^\alpha{}_{1j}$ and $M^\beta{}_{1j}$. Hence the total contribution of this type of diagram is $\sum_j M^\alpha{}_{1j}M^\beta{}_{1j}/\beta\omega_j^2$, so that the lowest order contribution to the susceptibility, $\chi_0^{\alpha\beta}$, Eq. (6), is

$$\chi_0^{\alpha\beta} = \tau^{-1}\sum_j M^\alpha{}_{1j}M^\beta{}_{1j}/\omega_j^2. \tag{16}$$

Note that this result is temperature-independent[13] and may also be obtained by considering the static equilibrium of the lattice in a constant field.

Next we consider all possible contributions to $\chi^{\alpha\beta}$ proportional to T, denoted by $\chi_1^{\alpha\beta}$. We restrict ourselves first to all diagrams which connect $M^\alpha{}_{1j}$ to $M^\beta{}_{1j'}$. Figures 2 and 3 are the only possible first- and second-order diagrams, respectively. Higher order diagrams will lead to a higher order temperature dependence.

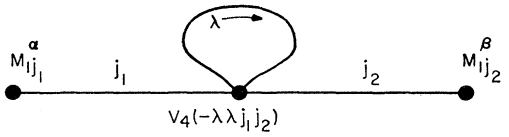

FIG. 2. A first-order diagram, the only contribution of the quartic potential to $\chi_1^{\alpha\beta}$.

[10] We will frequently use the word "diagram" to mean also "the term which the diagram represents." It should be clear from the context what is meant. Other topological words such as "line" or "vertex" may similarly have double meanings.

[11] There is a combinatorial consideration involved similar to the one of Appendix B.

[12] An alternative proof that only connected diagrams contribute to $\chi^{\alpha\beta} = (\partial P^\alpha/\partial E^\beta)_0$, as well as to higher derivatives of P^α, is as follows. From Appendix B, $\mathbf{P}$ [Eq. (3)] may be expressed in terms of only linked diagrams. [We now consider the V in Eq. (10) to be replaced by $V-\mathbf{E}\cdot\mathbf{M}$, so that there are internal vertices dependent upon $\mathbf{E}$, called $\mathbf{E}$ *vertices.*] Since there is only one external vertex, the linked diagrams are also connected diagrams. If such a diagram with n $\mathbf{E}$ vertices is differentiated with respect to E_β, it gives rise to a sum of connected diagrams with $(n-1)$ $\mathbf{E}$ vertices. Setting $\mathbf{E}=\mathbf{0}$, then, merely gets rid of all those diagrams for which $n\neq 1$, but of course the remaining ones are still connected.

[13] It is well known that the dielectric constant of a harmonic lattice is temperature independent. See, e.g., Fröhlich (Ref. 7) p. 170.

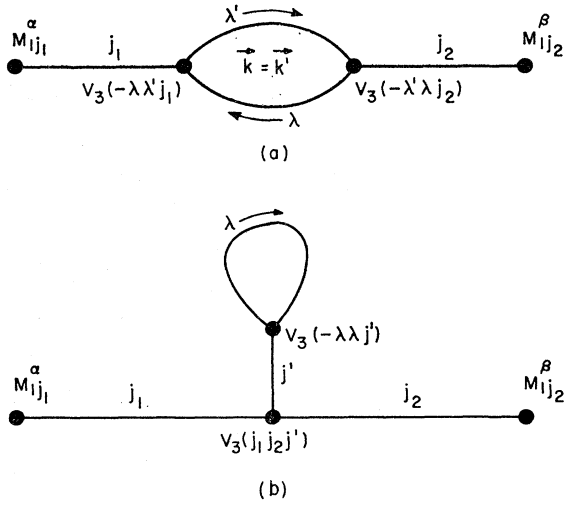

FIG. 3. The only two second-order diagrams which contribute to $\chi_1{}^{\alpha\beta}$. Diagram (b) vanishes for centro-symmetric crystals.

Figure 2-type diagrams contribute

$$12(-\beta/1!)\sum_{j1j2\lambda} M^{\alpha}{}_{1j1}M^{\beta}{}_{1j2}V_4(-\lambda\lambda j_1 j_2)g_{j1}g_{j2}g_{\lambda}. \quad (17)$$

The factor $(-\beta/1!)$ comes from the expansion of the exponential. The combinatorial factor 12 arises since each of the four modes in the expansion of V_4 Eq. (7d) may be paired with $M^{\alpha}{}_{1j1}$, while each of the three remaining modes may then be paired with $M^{\beta}{}_{1j2}$.[14]

Figure 3(a)-type diagrams contribute

$$36(\beta^2/2!)\sum_{\substack{j1j2\lambda\lambda' \\ \mathbf{k}=\mathbf{k}'}} M^{\alpha}{}_{1j1}M^{\beta}{}_{1j2} \times V_3(-\lambda\lambda' j_1)V_3(-\lambda'\lambda j_2)g_{j1}g_{j2}g_{\lambda}g_{\lambda'}. \quad (18)$$

The factor 36 arises since each of six modes in the two V_3's may be paired with $M^{\alpha}{}_{1j1}$, while each of three remaining modes may be paired with $M^{\beta}{}_{1j2}$. For each such combination there are two distinct ways of pairing the two remaining modes at each internal vertex.

Figure 3(b)-type diagrams contribute

$$36(\beta^2/2!)\sum_{j1j2j'\lambda} M^{\alpha}{}_{1j1}M^{\beta}{}_{1j2} \times V_3(j_1 j_2 j')V_3(-\lambda\lambda j')g_{j1}g_{j2}g_{j'}g_{\lambda}. \quad (19)$$

This contribution vanishes for centro-symmetric crystals since for such crystals[15]

$$V_3(-\lambda\lambda\lambda')\equiv 0. \quad (20)$$

Next we consider all diagrams which connect $M^{\alpha}{}_{1j1}$ to $M_2{}^{\beta}$ (and, of course, contribute to $\chi_1{}^{\alpha\beta}$). The only one, Fig. 4, contributes

$$6(-\beta/1!)\sum_{\substack{j1\lambda\lambda' \\ \mathbf{k}=\mathbf{k}'}} M^{\alpha}{}_{1j1}M_2{}^{\beta}(-\lambda\lambda')V_3(-\lambda'\lambda j_1)g_{j1}g_{\lambda}g_{\lambda'}. \quad (21)$$

The only diagram which connects $M^{\alpha}{}_{1j'}$ to $M_3{}^{\beta}$, Fig. 5, contributes

$$3\sum_{j'\lambda} M^{\alpha}{}_{1j'}M_3{}^{\beta}(-\lambda\lambda j')g_{j'}g_{\lambda}. \quad (22)$$

Of course, there are also contributions corresponding to Figs. 4 and 5 with the α and β indices interchanged.

The only diagram which connects $M_2{}^{\alpha}$ to $M_2{}^{\beta}$, Fig. 6, contributes

$$2\sum_{\substack{\lambda\lambda' \\ \mathbf{k}=\mathbf{k}'}} M_2{}^{\alpha}(-\lambda'\lambda)M_2{}^{\beta}(-\lambda\lambda')g_{\lambda}g_{\lambda'}. \quad (23)$$

From the above terms we thus find[16] for $\chi^{\alpha\beta}$, Eq. (6), neglecting terms of order T^2 and higher,

$$\chi^{\alpha\beta}=\chi_0{}^{\alpha\beta}+\chi_1{}^{\alpha\beta}, \quad (24)$$

where $\chi_0{}^{\alpha\beta}$ is given by Eq. (16) and $\tau\chi_1{}^{\alpha\beta}/(k_BT)$ equals

$$18\sum_{j1j2}\frac{M^{\alpha}{}_{1j1}M^{\beta}{}_{1j2}}{\omega_{j1}{}^2\omega_{j2}{}^2}\left\{\sum_{\substack{\lambda\lambda' \\ \mathbf{k}=\mathbf{k}'}}\frac{V_3(-\lambda\lambda' j_1)V_3(-\lambda'\lambda j_2)}{\omega_{\lambda}{}^2\omega_{\lambda'}{}^2}+\sum_{j'\lambda}\frac{V_3(j_1 j_2 j')V_3(-\lambda\lambda j')}{\omega_{j'}{}^2\omega_{\lambda}{}^2}\right\}-12\sum_{j1j2\lambda}\frac{M^{\alpha}{}_{1j1}M^{\beta}{}_{1j2}V_4(-\lambda\lambda j_1 j_2)}{\omega_{j1}{}^2\omega_{j2}{}^2\omega_{\lambda}{}^2}$$

$$+2\sum_{\substack{\lambda\lambda' \\ \mathbf{k}=\mathbf{k}'}}\frac{M_2{}^{\alpha}(-\lambda'\lambda)M_2{}^{\beta}(-\lambda\lambda')}{\omega_{\lambda}{}^2\omega_{\lambda'}{}^2}-6\sum_{\substack{j1\lambda\lambda' \\ \mathbf{k}=\mathbf{k}'}}\frac{V_3(-\lambda_0\lambda j_1)[M^{\alpha}{}_{1j1}M_2{}^{\beta}(-\lambda\lambda')+M^{\beta}{}_{1j1}M_2{}^{\alpha}(-\lambda\lambda')]}{\omega_{j1}{}^2\omega_{\lambda}{}^2\omega_{\lambda'}{}^2}$$

$$+3\sum_{j'\lambda}\frac{M^{\alpha}{}_{1j'}M_3{}^{\beta}(-\lambda\lambda j')+M^{\beta}{}_{1j1}M_3{}^{\alpha}(-\lambda\lambda j')}{\omega_{j'}{}^2\omega_{\lambda}{}^2}. \quad (25)$$

For a crystal with cubic symmetry, the dielectric susceptibility reduces to a scalar so that omitting the $\alpha\beta$ indices

[14] Note that the same factor applies also for the case where two or more mode pairs are the same. This will always be true.
[15] Reference 2, p. 2598.
[16] Equation (25) agrees with the classical static limit of Cowley's results (Ref. 2), when differences in definitions are taken into account, except that Cowley has apparently neglected to take into account our Fig. 3(b), and has left out a factor of 3 in his Eq. (6.11), which corresponds to our Eq. (22).

and using Eq. (20) we obtain

$$\chi_0=\tau^{-1}\sum_j M_{1j}^2/\omega_j^2, \tag{26}$$

$$\tau\chi_1/k_BT=2\sum_{\substack{\lambda\lambda'\\ \mathbf{k}=\mathbf{k}'}}\omega_\lambda^{-2}\omega_{\lambda'}^{-2}\Big|3\sum_{j1}\omega_{j1}^{-2}M_{1j1}V_3(-\lambda\lambda' j_1)-M_2(-\lambda\lambda')\Big|^2$$
$$-6\sum_{j1}\{\omega_{j1}^{-2}M_{1j1}\sum_\lambda\omega_\lambda^{-2}[2\sum_{j2}\omega_{j2}^{-2}M_{1j2}V_4(-\lambda\lambda j_1 j_2)-M_3(-\lambda\lambda j_1)]\}. \tag{27}$$

If Eq. (27) is specialized to the case of an alkali halide, so that only one optical mode contributes to the dipole moment along a crystalline axis, it agrees with the classical limit of Szigeti's quantum-mechanical formula[17] (when differences in definitions are taken into account). Equation (27) shows that cubic-potential terms and quadratic-dipole-moment terms contribute a positive temperature dependence to the dielectric susceptibility. Fuchs[18] observed this from the Szigeti

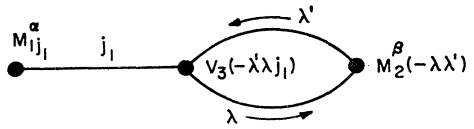

FIG. 4. This first-order diagram and a similar one with the α and β indices exchanged are the only contributions to $\chi_1^{\alpha\beta}$ which connect first- and second-order dipole-moment vertices.

formula[17] and showed also, making reasonable physical assumptions, that the quartic-potential and cubic-dipole-moment terms both contribute a negative temperature dependence. If Eq. (27) is specialized to a model in which each ion sits independently in a potential well of cubic symmetry, then, since the cubic-potential and quadratic-dipole-moment terms must vanish, a negative temperature dependence will result. Such a model has been used by Slater[30] in his theory of $BaTiO_3$. However, such a model cannot be used for the NaCl-type alkali halides, since it is experimentally known[18,19] that $(\partial\chi/\partial T)_V$ is positive.[20]

The validity of the perturbation expansion in powers of T is not known, but calculations[21] made to date suggest that it is valid at room temperature for a number of alkali halides. The relevant dimensionless expansion parameter is the mean-square amplitude ($\sim k_BT/\omega_\lambda^2$) divided by the square of some characteristic amplitude which is a measure of the onset of anharmonicity. We note that trouble can arise for modes having low frequencies, the so-called "soft modes." Although long-wavelength acoustical modes are of this type, they do not cause any trouble.[22] Of greater concern are soft optical modes, which we consider in the next section.

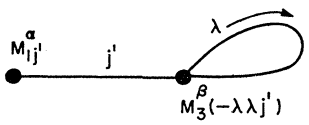

FIG. 5. This zeroth-order diagram and a similar one with the α and β indices exchanged are the only contributions to $\chi_1^{\alpha\beta}$ which connect first- and third-order dipole-moment vertices.

IV. TEMPERATURE-DEPENDENT FREQUENCIES AND PARAELECTRICS

As is well known, the presence of anharmonic terms causes the harmonic modes to interact. Hence the experimentally observed lattice-vibrational spectrum is not simply that of the temperature-independent harmonic frequencies ω_λ. Rather, following Cowley,[2] the spectrum may be considered to be due to a collection of independent harmonic oscillators with *temperature-dependent* frequencies $\bar{\omega}_\lambda$.

To define the $\bar{\omega}_\lambda$, we first introduce the *propagator*

$$G_{jj'}(\mathbf{k})\equiv\langle A_j(\mathbf{k})A_{j'}(-\mathbf{k})\rangle-\langle A_j(\mathbf{k})\rangle\langle A_{j'}(-\mathbf{k})\rangle \tag{28}$$
$$=G^*_{j'j}(\mathbf{k})=G^*_{jj'}(-\mathbf{k}) \tag{29}$$

by Eq. (9). (Note that for $\mathbf{k}\neq 0$, $\langle A_j(\mathbf{k})\rangle\equiv 0$, and that for $\mathbf{k}\neq\mathbf{k}'$, $\langle A_j(\mathbf{k})A_{j'}(-\mathbf{k}')\rangle\equiv 0$, which follow from the requirement of wave-vector conservation at every vertex.) It is clear from its definition that $G_{jj'}(\mathbf{k})$ is the sum of all diagrams which connect the external vertices $j\mathbf{k}$ and $j'-\mathbf{k}$. (We no longer require wave-vector conservation at the two external vertices.) In what follows, we will suppress the $\mathbf{k}$ dependence of the various quantities, e.g., $G_{jj'}\equiv G_{jj'}(\mathbf{k})$, but the implicit dependence upon $\mathbf{k}$ should be kept in mind. Figure 7 shows schematically how $G_{jj'}$ may be uniquely expressed as the sum of

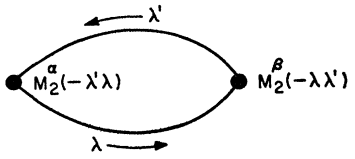

FIG. 6. The only contribution to $\chi_1^{\alpha\beta}$ from a diagram which connects two second-order dipole-moment vertices.

[17] B. Szigeti, Proc. Roy. Soc. (London) **A252**, 217 (1959), Eq. (4.21).
[18] R. Fuchs, MIT Laboratory for Insulation Research, Technical Report No. 167, p. 21, 1961 (unpublished).
[19] A. J. Boseman and E. E. Havinga, Phys. Rev. **129**, 1593 (1963).
[20] The above remarks are essentially those of Fuchs [Ref. (18)].
[21] R. M. Wilcox, National Bureau of Standards, Boulder Laboratories, 1964 (unpublished).
[22] The zero-wave-number acoustical modes correspond to a uniform translation of the lattice as a whole and hence do not affect any structural property of the crystal. See Ref. 17, p. 231.

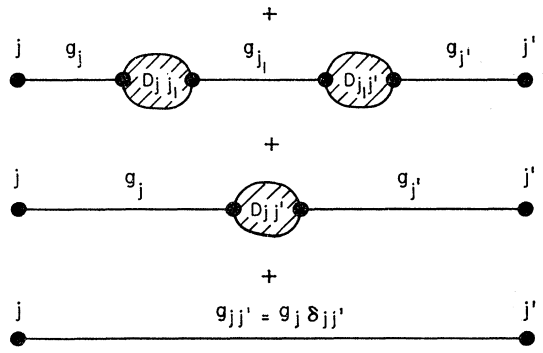

FIG. 7. The synthesis of the "propagator" $G_{jj'}$ from "lines" g_j and "bubbles" $D_{jj'}$.

different classes of diagrams. This may be written analytically[11]

$$G_{jj'}=g_{jj'}+g_jD_{jj'}g_{j'}+\sum_{j1}g_jD_{jj1}g_{j1}D_{j1j'}g_{j'}+\cdots, \quad (30)$$

where

$$g_{jj'}\equiv g_j\delta_{jj'}\equiv(\beta\omega_j^2)^{-1}\delta_{jj'}, \quad (31)$$

and the class of diagrams $D_{jj'}$ is called a *bubble*. The quantity $g_jD_{jj'}g_{j'}$ is defined to be the sum of all those diagrams for which the external vertices j and j' remain connected if any internal line is removed. If we write Eq. (30) in matrix form it is clear that it is simply the geometric series

$$\begin{aligned}G&=g+gDg+gDgDg+gDgDgDg+\cdots\\&\equiv g(1-Dg)^{-1}\equiv(1-gD)^{-1}g\equiv(g^{-1}-D)^{-1}.\end{aligned} \quad (32)$$

Since G is Hermitian, Eq. (29), it can be diagonalized by a (temperature-dependent) unitary matrix $\bar{U}$:

$$\bar{G}\equiv\bar{U}G\bar{U}^\dagger. \quad (33)$$

Since diagonal matrices are particularly easy to invert, $\bar{U}$ may be chosen such that $\bar{U}(g^{-1}-D)\bar{U}^\dagger$ is diagonal. Then Eqs. (32) and (33) show that $\bar{G}$ will be diagonal. By analogy with Eq. (31), we see that the temperature-dependent frequencies $\bar{\omega}_j$ should be defined by

$$\bar{G}_j\equiv(\beta\bar{\omega}_j^2)^{-1}. \quad (34)$$

The transformed temperature-dependent normal coordinates and potential should be defined, respectively, by

$$\bar{A}(\mathbf{k})\equiv\bar{U}(\mathbf{k})A(\mathbf{k}), \quad (35)$$

$$\bar{H}\equiv\tfrac{1}{2}\sum_\lambda\bar{\omega}_\lambda^2\bar{A}_\lambda^*\bar{A}_\lambda. \quad (36)$$

In Eq. (35), $A(\mathbf{k})$ represents a column matrix with elements $A_j(\mathbf{k})$, and we have again made explicit the dependence upon $\mathbf{k}$. Then Eqs. (28), (33), (34), and (35) imply that

$$\bar{G}_j=\langle|\bar{A}_j(\mathbf{k})|^2\rangle-\langle\bar{A}_j(\mathbf{k})\rangle^2 \quad (37)$$

$$=(\bar{A}_j(\mathbf{k})\bar{A}_j(-\mathbf{k}))_T \quad (38)$$

is the contraction symbol with respect to the temperature-dependent harmonic potential $\bar{H}$, Eq. (36).[23]

We next consider an alternative method for diagonalizing G which more closely parallels Cowley's "quasiharmonic approximation,"[2] and which is better suited to handle soft optical modes. We "renormalize" the potential $\mathfrak{U}$, Eq. (7), as follows:

$$\mathfrak{U}=\mathfrak{IC}+\mathfrak{V}, \quad (39)$$

$$\mathfrak{IC}\equiv H+Q, \quad (40)$$

$$\mathfrak{V}\equiv V-Q, \quad (41)$$

$$Q\equiv\tfrac{1}{2}\sum_{\mathbf{k}}A^\dagger(\mathbf{k})C(\mathbf{k})A(\mathbf{k})>0. \quad (42)$$

The positive-definite Hermitian matrix C will be determined later. The Hermitian matrix (ω^2+C) is diagonalized by a unitary matrix U:

$$\varpi^2\equiv U(\omega^2+C)U^\dagger\equiv U\omega^2U^\dagger+\hat{C}. \quad (43)$$

Defining

$$\mathfrak{A}=UA, \quad (44)$$

we see that

$$\mathfrak{IC}=\tfrac{1}{2}\sum_\lambda\varpi_\lambda^2\mathfrak{A}_\lambda^*\mathfrak{A}_\lambda, \quad (45)$$

and that the new contraction symbol, $(\mathfrak{A}_\lambda\mathfrak{A}_{\lambda'})$, will be given by

$$\hat{g}_{\lambda\lambda'}\equiv\delta_{-\lambda\lambda'}(\beta\varpi_\lambda^2)^{-1}. \quad (46)$$

Of course, $\mathfrak{V}$ must also be expressed in terms of the $\mathfrak{A}_\lambda$'s. From Eqs. (42), (43), and (44),

$$Q=\tfrac{1}{2}\sum_k\mathfrak{A}^\dagger(\mathbf{k})\hat{C}(\mathbf{k})\mathfrak{A}(\mathbf{k}). \quad (47)$$

Similarly, Eqs. (7c) and (7d), etc., are expressed in terms of the $\mathfrak{A}_\lambda$'s in a straightforward way to define new potential constants $\mathfrak{V}_3(\lambda\lambda'\lambda_2)$, $\mathfrak{V}_4(\lambda\lambda'\lambda_2\lambda_3)$, etc. The theory goes through the same as before so that corresponding to Eq. (32), we have

$$\mathbf{G}=\hat{g}(1-\mathbf{D}\hat{g})^{-1}. \quad (48)$$

The propagator $\mathbf{G}$ and the bubble $\mathbf{D}$ have the same topological definitions as before. Thus the same diagrams contribute to $\mathbf{D}$ as previously contributed to D, but in addition there is a contribution from $-Q$, Fig. 8. Consequently,

$$\mathbf{D}_{jj'}=\mathfrak{D}_{jj'}+\beta\hat{C}_{jj'}, \quad (49)$$

where $\mathfrak{D}$ is obtained from D by replacing g by $\hat{g}$ and by replacing the old potential constants $V_3(\lambda\lambda'\lambda_2)$, $V_4(\lambda\lambda'\lambda_2\lambda_3)$, etc., by the new temperature-dependent ones, $\mathfrak{V}_3(\lambda\lambda'\lambda_2)$, $\mathfrak{V}_4(\lambda\lambda'\lambda_2\lambda_3)$, etc., obtained by unitary

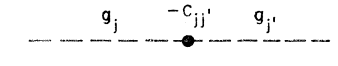

FIG. 8. The only new diagram to be included in the bubble $\mathbf{D}$. The dashed lines g_j and $g_{j'}$ are external to $\mathbf{D}$.

[23] Note that the unitary matrix $\bar{U}(-\mathbf{k})\equiv\bar{U}^*(\mathbf{k})$ diagonalizes $G(-\mathbf{k})$ with $\bar{G}(-\mathbf{k})=\bar{G}(\mathbf{k})$.

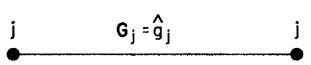

FIG. 9. The only diagram which contributes to $\mathbf{G}$.

transformation. We now require that

$$\hat{C} = -\beta^{-1}\mathfrak{D}. \tag{50}$$

Consequently $\mathbf{D}=0$, $\mathbf{G}=\hat{g}$, so that only the trivial diagram (Fig. 9) contributes to $\mathbf{G}$. Of course all of the quantities $\hat{g}$, $\mathcal{V}_3(\lambda\lambda'\lambda_2)$, $\mathfrak{D}$, etc., are implicit functions of $\hat{C}$, which is not known *a priori* but, at least in principle, $\hat{C}$ could be calculated by an obvious iterative procedure. Since $\mathbf{G}$ and $\bar{G}$ are both diagonal forms of the same matrix G, this method and the earlier method must give *essentially* the same results whenever both methods are valid. The nonuniqueness with respect to the choice of degenerate eigenvectors of G permits us to require

$$C_{jj'} = 0 \tag{51}$$

in the case where $\varpi_j = \varpi_{j'}$, $j \neq j'$, since this can always be obtained by a unitary transformation without altering $\mathbf{G}$.

If we neglect the nonlinear contributions to the dipole moment, the dielectric susceptibility is given entirely in terms of the temperature-dependent zero-wave number optical modes:

$$\chi^{\alpha\beta} = \tau^{-1}\sum_j \mathfrak{M}^{\alpha}{}_{1j}\mathfrak{M}^{\beta}{}_{1j}/\varpi_j{}^2 \tag{52}$$

$$= \tau^{-1}(\mathfrak{M}_1{}^{\alpha})^{\dagger}(\varpi^2)^{-1}\mathfrak{M}_1{}^{\beta}, \tag{52a}$$

where

$$\mathfrak{M}_1{}^{\alpha} = UM_1{}^{\alpha} = (\mathfrak{M}_1{}^{\alpha})^*. \tag{53}$$

Some of the apparent temperature dependence in Eq. (52) can be removed by writing Eq. (52a) in terms of the untransformed quantities using Eqs. (43) and (53),

$$\chi^{\alpha\beta} = \tau^{-1}(M_1{}^{\alpha})^{\dagger}(\omega^2+C)^{-1}M_1{}^{\beta}. \tag{54}$$

In Eq. (54), the temperature dependence occurs only in the matrix C, which is usually small compared to ω^2, We therefore break C up into its diagonal and nondiagonal parts $\mathcal{C}$ and $\bar{C}$, respectively,

$$C \equiv \mathcal{C}+\bar{C}, \tag{55}$$

and expand $(\omega^2+C)^{-1}$ in powers of $\bar{C}$,

$$(\omega^2+C)^{-1} = (\omega^2+\mathcal{C})^{-1} - (\omega^2+\mathcal{C})^{-1}\bar{C}(\omega^2+\mathcal{C})^{-1} + (\omega^2+\mathcal{C})^{-1}\bar{C}(\omega^2+\mathcal{C})^{-1}\bar{C}(\omega^2+\mathcal{C})^{-1} - \cdots. \tag{56}$$

When Eq. (56) is inserted into Eq. (54), the second term vanishes and

$$\chi^{\alpha\beta} = \tau^{-1}\sum_j \frac{M^{\alpha}{}_{1j}M^{\beta}{}_{1j}}{\omega_j{}^2+\mathcal{C}_j} + \tau^{-1}\sum_{jj_1j_2} \frac{M^{\alpha}{}_{1j}\bar{C}_{jj_1}\bar{C}_{j_1j_2}M^{\beta}{}_{1j_2}}{(\omega_j{}^2+\mathcal{C}_j)(\omega^2{}_{j_1}+\mathcal{C}_{j_1})(\omega^2{}_{j_2}+\mathcal{C}_{j_2})} + \cdots. \tag{57}$$

If

$$|C_{jj'}/\omega_j{}^2| < \lambda \ll 1 \tag{58}$$

for all j and j', then the second term in Eq. (57) is of order λ^2 relative to the first term (of order unity).

We now consider the case where there are one or more soft modes with frequency ϖ_0, $0<\varpi_0{}^2/\omega_j{}^2<\lambda$, and Eq. (58) still holds for j a nonsoft mode. Then, provided Eq. (51) is satisfied in the degenerate case, the second term of Eq. (57) will be of order λ relative to the first term, so that in this case

$$\chi^{\alpha\beta} = \tau^{-1}(\omega_0{}^2+\mathcal{C}_0)^{-1}\sum_j{}' M^{\alpha}{}_{1j}M^{\beta}{}_{1j}[1+\mathcal{O}(\lambda)]. \tag{59}$$

[The prime in Eq. (59) indicates that the sum is only over the soft modes.] For this case also,

$$\varpi_0{}^2 = (\omega_0{}^2+\mathcal{C}_0)[1+\mathcal{O}(\lambda)], \tag{60}$$

as may be seen from Eq. (43) by taking its determinant and using the fact that the determinant is invariant under unitary transformation. For this case also, we may assume that

$$U = e^{i\lambda B} = 1+i\lambda B+\mathcal{O}(\lambda^2), \tag{61}$$

where B is a Hermitian matrix of order unity. Consequently, Eq. (50) implies that

$$\mathcal{C}_0 = -k_BT\mathfrak{D}_{00}[1+\mathcal{O}(\lambda^2)]. \tag{62}$$

The main diagrams contributing to $\mathfrak{D}_{00}$ are Figs. 2 and 3 without the external lines and vertices. For a paraelectric material with cubic symmetry, Fig. 3(b) does not contribute and the dielectric susceptibility is a scalar. We thus find

$$\mathfrak{D}_{00} = -12\sum_{\lambda}\frac{\mathcal{V}_4(-\lambda\lambda 00)}{\varpi_\lambda{}^2} + 18\sum_{\substack{\lambda\lambda' \\ \mathbf{k}=\mathbf{k}'}}\frac{|\mathcal{V}_3(-\lambda\lambda' 0)|^2}{\varpi_\lambda{}^2\varpi_{\lambda'}{}^2}. \tag{63}$$

We see that $\mathfrak{D}_{00}$ is a temperature-dependent quantity, but that if the soft modes do not contribute too strongly to the sums in Eq. (63), $\mathfrak{D}_{00}$ will be approximately constant. Consequently, the well-known experimentally observed Curie law for the paraelectric susceptibility χ,

$$\chi = C/(T-T_C), \tag{64}$$

where C and T_C are positive constants, is implied by Eqs. (59), (62), and (63). The choice of signs indicates that an unstable harmonic mode, $\omega_0{}^2<0$, is stabilized by the quartic potential to make $\varpi_0{}^2>0$.[24]

Cowley[25] has experimentally studied the lowest fre-

[24] Note that since $\omega_0{}^2<0$ for this case, our earlier methods are not directly applicable since $\int \exp(-\frac{1}{2}\beta\omega_0{}^2A_0{}^2)dA_0$ then diverges. The "quasiharmonic approximation" may be looked upon as a method for analytically continuing our earlier solutions to smaller values of ω^2. However, for cases where the earlier methods are valid, they will be easier to apply, since they do not involve any iterative procedure. Previous statistical-lattice-dynamical derivations of equations like Eqs. (64) and (65) have been given by B. D. Silverman and R. I. Joseph, Phys. Rev. **129**, 2062 (1963); by Cowley (Ref. 2); and by Joseph and Silverman (Ref. 27). Most of our above remarks were made previously by these authors.

[25] R. A. Cowley, Phys. Rev. Letters **9**, 159 (1962). An earlier, less quantitative, indication that Eq. (65) was correct was obtained from the far-infrared-reflectivity measurements of A. S. Barker and M. Tinkham, Phys. Rev. **125**, 1527 (1962).

quency transverse-optical spectrum of $SrTiO_3$ by means of inelastic neutron scattering. He finds that this mode is well fitted by

$$\varpi_0^2 = C'(T - T_C), \tag{65}$$

which agrees with Eqs. (60), (62), and (63).

There is, however, an important difference between our derivations of Eqs. (64) and (65) and their experimental verifications, since the former are at constant volume, while the latter are at constant pressure. To apply our results to the constant-pressure case, we suppose that all lattice parameters are, to a good approximation, linear functions of the thermal expansion, hence also linear functions of the temperature. For the quantity $\mathfrak{D}_{00}$, Eq. (63), the fractional change will be negligible, but ω_0^2 may change appreciably. Hence the form of Eqs. (64) and (65) will be the same, but the constants C, T_C, and C' will be altered.[26]

V. FIELD-DEPENDENT SUSCEPTIBILITY

By taking higher derivatives of the polarization, analogous to Eq. (4), one can define field-independent nonlinear dielectric constants. This leads to connected[12] diagrams with more than two external vertices, such as have been calculated by Cowley.[2] These may be used to derive a generalization of the equation of state of Devonshire's thermodynamic theory of $BaTiO_3$, in the manner of Joseph and Silverman's[27] nondiagramatic classical theory. Instead of calculating nonlinear dielectric constants, however, we here prefer to calculate the more directly measurable field-dependent susceptibility $\chi^{\alpha\beta}(\mathbf{E})$ in a manner which emphasizes the field dependence of the soft optical modes.

Since Eq. (5) differs from Eq. (6) only by using a field-dependent ensemble rather than a field-independent ensemble, the preceding analysis applies with minor modifications. In Eqs. (10) and (11), V has to be replaced by $V(\mathbf{E}) \equiv V - \mathbf{M}\cdot\mathbf{E}$. We will consider only the contribution from the linear dipole moment $-\sum_j \mathbf{M}_{1j}\cdot\mathbf{E}A_j$. Equations (52) through (57) are still valid with $\chi^{\alpha\beta}$, ϖ, $\mathfrak{M}_1{}^\alpha$, and $\mathfrak{C}$ replaced, respectively, by $\chi^{\alpha\beta}(\mathbf{E})$, Ω, $\mathfrak{M}_1{}^\alpha$, and $\mathfrak{C}$, which are field-dependent as well

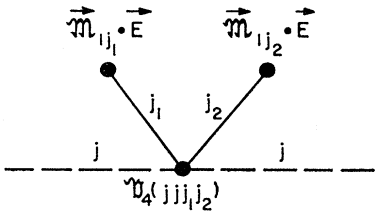

FIG. 10. A third-order diagram with two E vertices, a field-dependent contribution to the bubble $\mathfrak{D}$. The dashed g_j lines are external to $\mathfrak{D}$.

[26] Compare the thermodynamic treatment of A. F. Devonshire, in Advan. Phys. 3, 85 (1954), Sec. 4.2.1.

[27] R. I. Joseph and B. D. Silverman, Phys. Rev. A133, 207 (1964).

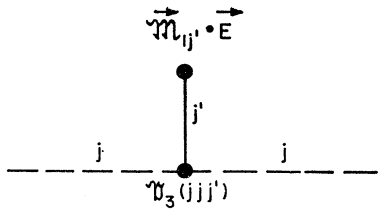

FIG. 11. A second-order diagram with one E vertex, a field-dependent contribution to the bubble $\mathfrak{D}$. The dashed g_j lines are external to $\mathfrak{D}$.

as temperature-dependent. (See Appendix C for more details.) Since the field may remove the degeneracy of the soft modes, it may no longer be possible to satisfy Eq. (51). However, provided Eq. (61) is still satisfied with a field-dependent $\mathfrak{B}$, then it is easy to show that Eq. (51) is replaced by $C_{jj'}(\mathbf{E}) = [\mathcal{O}(\lambda)]\Omega_j^2$. [See Eqs. (C11) and (C12).] Hence, our previous conclusion that the second term in Eq. (57) is of order λ relative to the first is still valid. We thus have, corresponding to Eqs. (59) and (60),

$$\chi^{\alpha\beta}(\mathbf{E}) = [1+\mathcal{O}(\lambda)]\tau^{-1}\textstyle\sum_j' M^\alpha{}_{1j}M^\beta{}_{1j}/\Omega_j^2, \tag{66}$$

and

$$\Omega_j^2 = (\omega_0^2 + \mathfrak{C})[1+\mathcal{O}(\lambda)]. \tag{67}$$

Although $\chi^{\alpha\beta}(\mathbf{E})$ reduces to a scalar χ for a crystal with cubic symmetry in the absence of a biasing field $\mathbf{E}$, Eq. (66) shows that this need not be the case if the field splits the degenerate soft modes. In analogy with Eq. (62),

$$\mathfrak{C}_j = -k_B T\mathfrak{D}_{jj}[1+\mathcal{O}(\lambda^2)] \tag{68}$$

where

$$\mathfrak{D} = \mathfrak{D} + \bar{\mathfrak{D}}. \tag{69}$$

The quantity $\mathfrak{D}_{jj}$ comes from the same diagrams which contributed to the field-off case, and is approximately the same as $\mathfrak{D}_{00}$ Eq. (63):

$$\mathfrak{D}_{jj} = \mathfrak{D}_{00}[1+\mathcal{O}(\lambda)]. \tag{70}$$

The quantity $\bar{\mathfrak{D}}$, on the other hand, is the contribution from $\mathbf{E}$-vertex diagrams, the most important of which are shown in Figs. 10 and 11. From Eqs. (67), (68), (69) (70), and (62), it follows that

$$\Omega_j^2 = \varpi_0^2 - \beta^{-1}\bar{\mathfrak{D}}_{jj} \tag{71}$$

for a soft mode j. The contribution of Fig. 10 to $\bar{\mathfrak{D}}_{jj}$ is

$$-12\beta\sum_{j_1j_2}\frac{\mathfrak{V}_4(jjj_1j_2)(\mathfrak{M}_{1j_1}\cdot\mathbf{E})(\mathfrak{M}_{1j_2}\cdot\mathbf{E})}{\Omega_{j_1}^2\Omega_{j_2}^2}. \tag{72}$$

The contribution of Fig. 11 to $\bar{\mathfrak{D}}_{jj}$ is

$$6\beta\textstyle\sum_{j'}\mathfrak{V}_3(jjj')(\mathfrak{M}_{1j'}\cdot\mathbf{E})/\Omega_{j'}^2. \tag{73}$$

Although $\mathfrak{V}_3(jjj')$ vanishes for a centro-symmetric crystal when the biasing field is turned off, Eq. (20), it need not vanish when the field is on. When the field is

on, $\mathfrak{V}_3(j'j'j'')$ will be a linear combination of the average amplitudes $\langle\mathfrak{A}_j\rangle_E$ with approximately constant coefficients. Since a simple calculation[28] shows that, to lowest order, $\langle\mathfrak{A}_j\rangle_E=\mathfrak{M}_{1j}\cdot\mathbf{E}/\Omega_j^2$, Eq. (73) is actually of the same form as Eq. (72). Consequently, $\bar{\mathfrak{D}}_{jj}$ is given entirely (to the order of our approximation) by Eq. (72) with the approximately constant coefficients $\mathfrak{V}_4(jjj_1j_2)$ redefined appropriately.

In the remainder, we will consider two special cases: (a) the biasing field does not appreciably split the soft modes, so that

$$\Omega_j^2\cong\Omega^2 \tag{74}$$

for all such modes, and the dielectric tensor Eq. (66) is still approximately a scalar,

$$\chi(\mathbf{E})=\bar{C}/\Omega^2, \tag{75}$$

where $\bar{C}$ is constant to order λ; (b) the degeneracy is substantially removed by the biasing field (assumed to be in the z direction), but only one mode appreciably contributes to the z component of the dipole moment. In case (a), Eqs. (71), (72), and (74) then imply that

$$\Omega^2=\varpi_0^2+\bar{A}(\hat{e})E^2/\Omega^4, \tag{76}$$

where $\bar{A}(\hat{e})$ depends only (to order λ) upon the direction $\hat{e}$ of the biasing field $\mathbf{E}$. From Eqs. (75) and (76), one finds

$$\chi(\mathbf{E})=\chi[1+A(\hat{e})\chi\chi^2(\mathbf{E})E^2]^{-1}, \tag{77}$$

where $A(\hat{e})\equiv\bar{A}(\hat{e})/\bar{C}^3$ is a quantity like $\bar{A}(\hat{e})$, and $\chi=\bar{C}/\varpi_0^2$ is the susceptibility with the biasing field turned off, Eq. (64).[29] In case (b), Eq. (66) for $\chi^{zz}(E_z)$ and Eq. (72) each reduce to a single term, so that we again obtain Eq. (77) with $\chi(\mathbf{E})$ replaced by $\chi^{zz}(E_z)$. It therefore appears likely that Eq. (77) will apply well to the (100) direction of paraelectric perovskites, such as $SrTiO_3$.

If $\mathbf{E}$ is so small that $\chi(\mathbf{E})\cong\chi$, Eq. (77) may be approximated by

$$\chi(\mathbf{E})=\chi[1+A(\hat{e})\chi^3E^2]^{-1}. \tag{78}$$

An equation equivalent to Eq. (78), based upon the Slater theory[30] of ferroelectricity in perovskite structures, has been experimentally verified for the (100), (110), and (111) directions of $SrTiO_3$ by Rupprecht, Bell, and Silverman.[31] In contrast to our theory, however, the Slater theory assumed an ionic independent-well model.[32]

From the point of view of the theory presented here, Eq. (77) should be at least as accurate as Eq. (78). However, it is not yet known which formula better fits experiments. Since Eq. (77) is a cubical equation in $\chi(\mathbf{E})$, an explicit expression can be obtained if desired. However, to experimentally determine the range of validity of Eq. (77) or (78), it will be preferable to solve for $A(\hat{e})$ and observe the constancy of the resulting expression as E or T is varied. In the same way, the constancy of $\bar{A}(\hat{e})$ in Eq. (76) can be determined by extending the inelastic neutron-scattering experiments of Cowley[25] to consider field dependence[33] as well as temperature dependence.

ACKNOWLEDGMENT

The author is indebted to Dr. Solomon J. Glass for referring him to the Cowley article,[2] and for other useful remarks made prior to the start of this investigation.

APPENDIX A: PROOF OF EQS. (14)

The integrations implied in Eqs. (12) and (13) could be carried out using the real and the imaginary parts of the A_λ's as independent variables, but it is preferable to transform to polar coordinates R_λ, θ_λ as follows:

$$\left.\begin{aligned}&A_\lambda\equiv 2^{-1/2}R_\lambda\exp(i\theta_\lambda),\\ &A_{-\lambda}=(A_\lambda)^*\equiv 2^{-1/2}R_\lambda\exp(-i\theta_\lambda),\end{aligned}\right\}\mathbf{k}\neq 0,\qquad A_\lambda=(A_\lambda)^*\equiv R_\lambda,\quad \mathbf{k}=0, \tag{A1}$$

and $d\tau=\text{const}\ d\tau_0R_1dR_1R_2dR_2\cdots R_ndR_nd\theta_1d\theta_2\cdots d\theta_n$, where $d\tau_0$ is the volume element associated with the $\mathbf{k}=\mathbf{0}$ modes. When Eqs. (A1) are substituted into Eq. (7a), the harmonic potential becomes $H=\frac{1}{2}\sum_\lambda\omega_\lambda^2R_\lambda^2$ with the summation restricted to half of the first Brillouin zone. By writing $e^{-\beta H}$ as a product of the factors $\exp(-\frac{1}{2}\beta\omega_\lambda^2R_\lambda^2)$, the integrations may be done independently by using the following integrals:

$$\int_0^{2\pi}e^{in\theta}d\theta=\delta_{n0}\int_0^{2\pi}d\theta; \tag{A2a}$$

$$\int_0^\infty R^{2n}[\exp(-\tfrac{1}{2}\beta\omega^2R^2)]RdR=n!(\beta\omega^2)^{-n}\int_0^\infty[\exp(-\tfrac{1}{2}\beta\omega^2R^2)]RdR; \tag{A2b}$$

$$\int_{-\infty}^\infty R^{2n-1}[\exp(-\tfrac{1}{2}\beta\omega^2R^2)]dR=0; \tag{A2c}$$

[28] This is obtained from a simple diagram like that of Fig. 1, but with different vertices. One, an external vertex, comes from the $\mathfrak{A}_j$, while the other, an internal vertex, comes from the jth mode contribution to $-\mathbf{M}\cdot\mathbf{E}$ in $\mathfrak{V}$.

[29] Arguments similar to those of the last paragraph of Sec. IV show that the quantities $\bar{C}$, $\bar{A}$, and A should not be appreciably altered by thermal expansion. Hence our equations should apply to constant pressure as well as constant volume experiments.

[30] J. C. Slater, Phys. Rev. **78**, 748 (1950).

[31] G. Rupprecht, R. O. Bell, and B. D. Silverman, Phys. Rev. **123**, 97 (1961).

[32] Since our theory is essentially model independent, the difference between Eq. (77) and the Slater-theory formula cannot be attributed to Slater's choice of model. The difference must thus be due entirely to the difference methods of approximation used in the two theories.

[33] The extension of such experiments to the field-dependent case has been frequently discussed by many workers in the field. A treatment of the field dependence of a soft-mode frequency in Cochran's theory of ferroelectricity has been given by E. Fatuzzo, Proc. Phys. Soc. (London) **84**, 709 (1964).

$$\int_{-\infty}^{\infty} R^{2n}[\exp(-\tfrac{1}{2}\beta\omega^2R^2)]dR = (2n-1)!!(\beta\omega^2)^{-n}\int_{-\infty}^{\infty}[\exp(-\tfrac{1}{2}\beta\omega^2R^2)]dR. \quad \text{(A2d)}$$

From Eqs. (A2a, A2c) it follows that $(\lambda_1,\lambda_2\cdots\lambda_n)$ vanishes unless it is possible to separate the λ_i into disjoint pairs λ, λ' such that $\lambda=-\lambda'$. This will always be the case if n is odd, which proves Eq. (14a). The contraction symbol, Eq. (14c), evidently follows as a special case of Eqs. (A2). Equation (14b) may be verified from Eqs. (A2) as follows. If it is not possible to separate the λ_i into disjoint pairs λ, λ' with $\lambda=-\lambda'$, then evidently both sides vanish. If all of the $2n$ λ_i's are equal, the only nonvanishing case is for $\mathbf{k}=0$. By Eq. (A2d), the left-hand side is then given by $(2n-1)!!(\beta\omega_\lambda{}^2)^{-1}$, while each of the $(2n-1)!!$ terms[34] of the right-hand side equals $(\beta\omega_\lambda{}^2)^{-n}$. For the case $(\lambda\lambda\cdots\lambda\,-\lambda\,-\lambda\cdots-\lambda)$, with n λ's and n $-\lambda$'s, Eq. (A2b) shows that the left-hand side equals $n!(\beta\omega_\lambda{}^2)^{-n}$, while there are exactly $n!$ nonvanishing terms[35] on the right-hand side, each equal to $(\beta\omega_\lambda{}^2)^{-n}$. For the case in which there are a number of kinds of $(-\lambda\lambda)$ pairs, both sides of Eq. (14b) factor into products of the above type. For the left-hand side this follows from the independence of the integrals over different variables, while for the right-hand side this follows from the fact that $(\lambda\lambda')=0$ for $\lambda'\neq-\lambda$. A more formal proof of Eq. (14b) may be given by the method of mathematical induction.

APPENDIX B: LINKED-DIAGRAM THEOREM

Equations (10) and (11) are of the form N/D with

$$N\equiv\sum_{n=0}^{\infty}N_n/n!, \quad \text{(B1)}$$

$$D\equiv 1+\sum_{n=1}^{\infty}D_n/n!, \quad \text{(B2)}$$

where N_n is the sum of all diagrams having n internal vertices and a fixed number of external vertices, while D_n is the sum of all diagrams having n internal vertices and no external vertices. Now

$$N_n=\bar{N}_n+\hat{N}_n, \quad \text{(B3)}$$

where $\bar{N}_n$ and $\hat{N}_n$ are, respectively, the sums of all linked and unlinked diagrams of order n. Now each unlinked diagram is equivalent to a linked diagram of lower order multiplied by a diagram of D, and $\hat{N}_n$ must be the sum of all possible products with n internal vertices. Hence

$$\hat{N}_n=\sum_{j=0}^{n-1}\frac{n!\bar{N}_jD_{n-j}}{j!(n-j)!}. \quad \text{(B4)}$$

The combinatorial factor $n!/[j!(n-j!)]$ occurs since it is the number of ways of assigning j internal vertices to $\bar{N}_j$ and $(n-j)$ remaining vertices to D_{n-j}. Substituting Eqs. (B3) and (B4) into Eq. (B1), we obtain

$$N=\bar{N}+\sum_{n=0}^{\infty}\sum_{j=0}^{n-1}\frac{\bar{N}_jD_{n-j}}{j!(n-j)!}, \quad \text{(B5)}$$

where

$$\bar{N}\equiv\sum_{n=0}^{\infty}\bar{N}_n/n! \quad \text{(B6)}$$

is the sum of all linked diagrams. The double sum in Eq. (B5) is the same as

$$\sum_{n=0}^{\infty}\sum_{j=1}^{\infty}\frac{\bar{N}_n}{n!}\frac{D_j}{j!}=\bar{N}(D-1), \quad \text{(B7)}$$

by Eqs. (B2) and (B6). Hence $N/D=\bar{N}$. Q.E.D.

APPENDIX C: SOME DETAILS OF THE FIELD-DEPENDENT CALCULATION

Since the general topological considerations of Secs. III and IV are independent of the detailed nature of the potential, they still apply to the field-dependent calculation. A field-dependent propagator $G(\mathbf{E})$ is defined the same as G in Eq. (28) except that the ensemble averages are now field-dependent [in the sense of Eq. (2)]. The propagator $G(\mathbf{E})$ is still the sum of all connected diagrams, but this now includes new, $\mathbf{E}$-vertex diagrams not present previously. The propagator $G(\mathbf{E})$ is again diagonalized by the renormalization method so that instead of Eqs. (39)–(42) we have, respectively

$$\mathfrak{U}=\mathfrak{H}+\mathfrak{V}, \quad \text{(C1)}$$

$$\mathfrak{H}=H+Q', \quad \text{(C2)}$$

$$\mathfrak{V}\equiv V(\mathbf{E})-Q', \quad \text{(C3)}$$

$$Q'\equiv\tfrac{1}{2}\textstyle\sum_k A^\dagger(\mathbf{k})C'(\mathbf{k})A(\mathbf{k})>0. \quad \text{(C4)}$$

In analogy to Eq. (43), a unitary matrix U' is found which diagonalizes (ω^2+C')

$$\Omega^2\equiv U'(\omega^2+C')(U')^\dagger\equiv U'\omega^2(U')^\dagger+\hat{C}', \quad \text{(C5)}$$

and thus defines Ω. In analogy to Eq. (44), the temperature-dependent amplitudes $\mathfrak{A}_j$ are defined by

$$\mathfrak{A}=U'A. \quad \text{(C6)}$$

The algebraic and topological considerations involved in the analogs of Eqs. (45)–(50) are formally the same as previously, so that in place of Eq. (50) we obtain

$$\hat{C}'=-\beta^{-1}\mathfrak{D} \quad \text{(C7)}$$

where the bubble $\mathfrak{D}$ includes new, $\mathbf{E}$-vertex diagrams not present previously. The diagrams contributing to $\mathfrak{D}$ are to be calculated with the field- and temperature-

[34] The number of distinct ways of pairing $2n$ objects with each other is $(2n-1)!!\equiv(2n)!/(2^nn!)$.

[35] The number of distinct ways of pairing two sets, each of which contains n objects, is $n!$.

dependent propagators ($\beta^{-1}\Omega_j^{-2}$) and with new dipole-moment and potential constants $\mathfrak{M}_{1j}$, $\mathfrak{V}_3(\lambda\lambda'\lambda'')$, etc., obtained from the original ones M_{1j}, $V_3(\lambda\lambda'\lambda'')$, etc., by unitary transformation with the matrices $U'(\mathbf{k})$. In analogy to Eq. (52), we have

$$\chi^{\alpha\beta}(\mathbf{E})=\tau^{-1}\sum_j \mathfrak{M}^{\alpha}{}_{1j}\mathfrak{M}^{\beta}{}_{1j}/\Omega_j^2. \quad \text{(C8)}$$

As previously, some of the apparent field and temperature dependence may be transformed away so that, corresponding to Eq. (54),

$$\chi^{\alpha\beta}(\mathbf{E})=\tau^{-1}(M_1{}^{\alpha})^{\dagger}(\omega^2+C')^{-1}M_1{}^{\beta}. \quad \text{(C9)}$$

As in Eq. (55), the matrix C' is broken up into its diagonal and nondiagonal parts $\mathfrak{C}$ and $\tilde{C}'$, respectively.

$$C'=\mathfrak{C}+\tilde{C}', \quad \text{(C10)}$$

and expanded as in Eq. (56). In place of Eq. (61), we assume that

$$U'=\exp(i\lambda\mathfrak{B})=1+i\lambda\mathfrak{B}+\mathcal{O}(\lambda^2), \quad \text{(C11)}$$

where $\mathfrak{B}$ is of order unity. Equation (67) then follows by substituting Eqs. (C10) and (C11) into Eq. (C5), taking diagonal elements, and using the fact that $[\mathfrak{B},\omega^2]_{jj}=0$.

To obtain the matrix element $C'_{jj'}$ between two formerly degenerate soft-mode states j and j', first solve Eq. (C5) for C', then substitute Eq. (C11). The result is

$$C'_{jj'}=i\lambda[\Omega^2,\mathfrak{B}]_{jj'}=i\lambda\mathfrak{B}_{jj'}(\Omega_j^2-\Omega_{j'}^2)$$
$$=\mathcal{O}(\lambda)\Omega_j^2=\mathcal{O}(\lambda)\Omega_{j'}^2. \quad \text{(C12)}$$

We further assume, in analogy to Eq. (58), that for j a nonsoft mode

$$|C'_{jj'}/\omega_j^2|<\lambda\ll 1. \quad \text{(C13)}$$

Also, if j' and j are soft and nonsoft modes, respectively, we require that

$$0<\Omega_{j'}^2/\omega_j^2<\lambda. \quad \text{(C14)}$$

If Eqs. (C12), (C13), (C14), and (67) are substituted into the analog of Eq. (57), Eq. (66) results.

PHYSICAL REVIEW VOLUME 139, NUMBER 4A 16 AUGUST 1965

Hybrid Excitons in Diamond*

J. C. PHILLIPS†‡
Bell Telephone Laboratories, Murray Hill, New Jersey
(Received 5 October 1964)

The fundamental reflectivity spectrum of type-IIa diamond has been studied recently by several workers. Our purpose here is to discuss the edge at 7.1 eV which has previously been assigned to the direct threshold $\Gamma_{25}'\rightarrow\Gamma_{15}$. We show instead that a hybrid exciton is present near 7 eV, and that the direct threshold probably occurs at about 8.7 eV. The implications of the revised interpretation for the electronic structure of diamond are also discussed.

1. INTRODUCTION

THE indirect and direct energy gaps in diamond are similar to those in Si. The indirect gap arises from transitions between $\Gamma_{25'}$ and the bottom of the conduction band near X_1, and occurs at 1.1 and 5.5 eV in Si and C, respectively. The direct gap in Si occurs near 3.5 eV. However, while the line shape neglecting exciton effects is predicted to resemble a step function, the experimental room-temperature spectrum exhibits a peak.[1,2] The peak in Si has been explained tentatively as an exciton[3] (see Fig. 1).

The fundamental reflectivity spectrum of diamond has been measured recently by several workers.[4,5] In all cases the optical measurements appear reliable, but rather large differences are found in the observed reflectivity. For example, the percentage reflectance at the largest peak near 12.6 eV is found to be 62%,[4] or 52%,[6] or 42%.[5] Large *qualitative* differences in line shape are found near the 7-eV "direct edge." We believe that at least some of these differences are a result of varying degrees of roughness at the surface of each sample,[5] and that these conditions drastically alter the lifetimes of exciton resonances. In particular, we

* Supported in part by the National Science Foundation and the National Aeronautics and Space Administration.
† A. P. Sloan Fellow.
‡ Permanent address: Department of Physics, University of Chicago, Chicago, Illinois.
[1] See the experimental data of H. R. Philipp quoted in Ref. 2.
[2] D. Brust, Phys. Rev. **134**, A1337 (1964); also D. Brust, Marvin L. Cohen, and J. C. Phillips, Phys. Rev. Letters **9**, 389 (1962).
[3] J. C. Phillips, Phys. Rev. Letters **10**, 329 (1963).
[4] H. R. Philipp and E. A. Taft, Phys. Rev. **127**, 159 (1962).
[5] C. D. Clark, P. J. Dean, and P. V. Harris, Proc. Roy. Soc. (London) **A277**, 312 (1964); P. J. Dean (private communication). Dr. Dean reports that the best data shown in Fig. 2 used a natural surface. The best polished surface "was examined by multiple-beam interferometry. The surface was found to be very flat, but polishing marks about 10–20-μ wide and 150-Å deep were detected. Small percussion marks were also revealed under $\times 1200$ magnification which were in small clusters across the surface of the specimen. Freshly cleaved samples showed steps visible to the naked eye."
[6] W. C. Walker and J. Osantowski, Phys. Rev. **134**, A153 (1964).